

High-Pressure High-Resolution Nuclear Magnetic Resonance III: Concentration Dependence of ΔV^\ddagger and ΔG^\ddagger for the Rotation of the Dimethylaminogroup in Aqueous Solutions of Some N,N-Dimethylamides

G. Völkel, E. Lang, and H.-D. Lüdemann

Institut für Biophysik und Physikalische Biochemie, Universität Regensburg, Postfach 397, D-8400 Regensburg

Biophysikalische Chemie / Flüssigkeiten / Hohe Drücke / Magnetische Kernresonanz

The concentration dependence of the activation volume ΔV^\ddagger and the free activation enthalpy ΔG^\ddagger for the inversion of the dimethylaminogroup has been determined in a series of dimethylamides in aqueous solution by high pressure HRNMR ($p_{\max} = 150$ MPa). The compounds studied are the N,N-dimethylamides of formic-, acetic-, propionic-, isobutyric-, valerianic- and benzoic acid. In all nonaqueous solvents ΔV^\ddagger is only slightly concentration dependent, ΔV^\ddagger being in the range of $+10 \pm 2 \text{ cm}^3 \cdot \text{mol}^{-1}$. For all compounds studied, ΔV^\ddagger in the dilute aqueous solutions ($x_{\text{D}_2\text{O}} \geq 0.9$) decreases very rapidly to values around $+2 \text{ cm}^3 \cdot \text{mol}^{-1}$. It is attempted to explain this decrease by the formation of an open hydration shell around the dimethylaminogroup and to correlate the concentration effects with the hydrophobic character of the amides.

Für eine Reihe von N,N-Dimethylamiden wurde in wäßriger Lösung die Konzentrationsabhängigkeit des Aktivierungsvolumens ΔV^\ddagger und der freien Aktivierungsenthalpie ΔG^\ddagger für die Inversion der Dimethylaminogruppe aus der Druck- und Temperaturabhängigkeit der Protonenhochauflösungsspektren bestimmt ($p_{\max} = 150$ MPa). Die untersuchten Systeme sind die N,N-Dimethylamide der Ameisen-, Essig-, Propion-, Isobutter-, Valerian- und Benzoesäure. In allen nichtwäßrigen Lösungsmitteln ist ΔV^\ddagger nur sehr wenig von der Konzentration abhängig und liegt im Intervall $+10 \pm 2 \text{ cm}^3 \cdot \text{mol}^{-1}$. In den verdünnten wäßrigen Lösungen ($x_{\text{D}_2\text{O}} \geq 0.9$) aller angegebenen Amide dagegen nimmt ΔV^\ddagger sehr rasch auf Werte um $+2 \text{ cm}^3 \cdot \text{mol}^{-1}$ ab. Es wird versucht, diese Abnahme durch die Bildung einer offenen Hydrathülle um die Dimethylaminogruppe zu erklären und die in den einzelnen Systemen unterschiedliche Konzentrationsabhängigkeit über die hydrophobe Wechselwirkung zu beschreiben.

Introduction

In a previous paper [1] the solvent dependence of the activation volume ΔV^\ddagger for the hindered internal rotation of the dimethylaminogroup in a series of simple N,N-dimethylamides was studied with a recently developed technique for the determination of ΔV^\ddagger by variable temperature high pressure HRNMR [2, 3]. The results found for a wide variety of solvents, showed a remarkable independence of ΔV^\ddagger from the properties of the solvent.

It is well established, that ΔG^\ddagger increases with the polarity of the solvent [4–6]. The effect is most pronounced for protic solvents like water and methanol and is explained by a preferred stabilisation of the highly polar ground state through the interaction with the dipoles of the solvent. The influence of the solvent polarity upon the activation volume was studied in a wide variety of solvents (CCl_4 , C_6D_6 , $(\text{CD}_3)_2\text{CO}$, $(\text{CD}_3)_2\text{SO}$, CD_3CN , CD_3OD , D_2O) [1]. No significant effect was found. In all solvents ΔV^\ddagger is around $10 \text{ cm}^3 \cdot \text{mol}^{-1}$. Only the aqueous solutions of dimethylformamide and dimethylacetamide revealed significantly lower ΔV^\ddagger . The most surprising result being found in the 20 v/v-% aqueous solution of dimethylacetamide, where the rate of inversion for the dimethylaminogroup is almost unaffected by the increase of hydrostatic pressure and described by an activation volume of $1.6 \text{ cm}^3 \cdot \text{mol}^{-1}$. The most probable explanation for this finding has to be searched for in the unique structural characteristics of the solvent water. We therefore started a systematic study of the concentration dependence of ΔV^\ddagger and ΔG^\ddagger in a series of N,N-dimethylamides in aqueous solution. The dimethylamides of the following aliphatic carbonic acids were studied: formic-,

acetic-, propionic-, isobutyric-, valerianic- and hexanoic acid. Within this series the unpolar substituent of the carbonyl carbon increases, thus enhancing the possibility and extent of hydrophobic interaction between this part of the solute molecules. Dimethylhexanoicamide is the bulkiest member of this series and possesses only very limited solubility in water. The dimethylamides of the higher fatty acids are only very sparingly soluble in water, the solubility decreasing with rising temperature. In addition the aqueous solutions of dimethylbenzamide were investigated.

The close structural similarity between the dimethylamidegroup and the peptidegroup as the building block of the proteins makes it very plausible, that the results obtained in these model systems are also of relevance for the natural aqueous solutions of enzymes and structural proteins.

Materials and Methods

Materials

N,N-dimethylformamide (DMF) (Uvasol, E. Merck, Darmstadt, FRG), N,N-dimethylacetamide (DMA) (puriss., Fluka, Buchs, Switzerland), N,N-dimethylbenzamide (DMB) (ICN, Serva, Heidelberg, FRG) are commercial products and were used without further purification. N,N-dimethylpropionamide (DMP), N,N-dimethylvalerianamide (DMV), and N,N-dimethylhexanamide (DMHex) were prepared from the respective carbonylchlorides dissolved in dried dioxane, by slow addition of a surplus of dimethylamine. In N,N-dimethylisobutyramide (DMiBu) the signal from the α -proton overlaps with the two N-methyl signals. The α -deuterated dimethylamide was prepared from α -bromo-isobutyric ethylester (EGA-Chemie, Steinheim/Albuch, FRG) by published procedures [7]. The dimethylamides were purified by fractional vacuum distillation over a Vigreux column. Deuteriumoxyde 99.7% deuterated (E. Merck, Darmstadt, FRG) was used in the solutions. The solutions

were prepared by weighing. In order to provide for all solutions a strong, sharp proton signal for internal locking and shimming, a part of the heavy water was replaced by triple distilled light water. Details of the compositions are given in the tables.

Experimental

Fig. 1 gives the schematic of the high pressure high resolution NMR cell. The cell is a strongly modified version of the strengthened glass cell design introduced by Yamada [8]. Compared to our first modification [9, 10] the handling is further facilitated by protecting the upper end of the glass capillary, after shrink fitting of the teflon hose, with a thinwalled brass tube filled with epoxy resin.

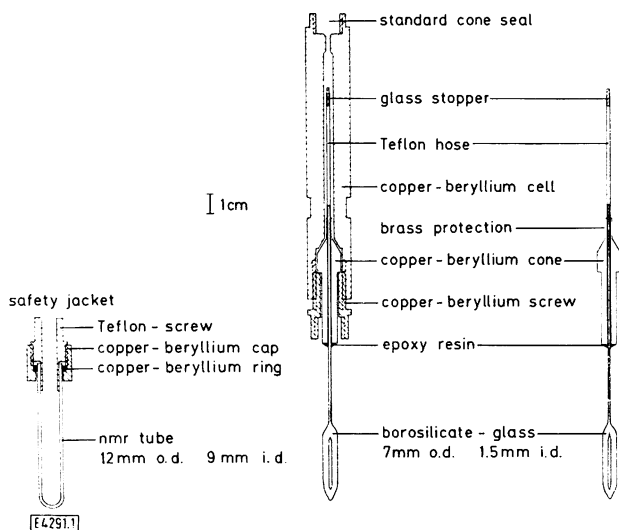


Fig. 1
High pressure NMR-cell

This cell fits into the standard 12 mm probe of a Varian XL-100-15-FT-NMR-spectrometer. The spinner housing of the probe is replaced by a coolable aluminum holder. Intensive cooling of this holder keeps the epoxy connection between glass cell and metal nipple near room temperature, even at 450 K in the main solution container.

The temperature was regulated with the standard variable temperature accessory and controlled to ± 0.5 K with a miniature thermocouple.

Spectra

The spectra were obtained in the FT mode (Varian 620-1-100 16 k computer with interactive disk accessory). The shimming of the magnetic field was achieved while locking the spectrometer to a strong proton signal of the high pressure cell content. During spectra accumulation the spectrometer was locked to an external ^{19}F -lock. Typical spectra are given in Fig. 2. In the region of the coalescence temperature T_c , 10 to 15 isotherms spaced approximately by 1 K were determined. Simulation of the exchange broadened spectra was done either by application of the DNMR-5 program [11] or using an experimental line shape analysis program [12]. The chemical shift difference $\Delta\nu$ in the temperature region of chemical exchange broadening was determined from a linear extrapolation of the $\Delta\nu$ measured 30 to 50 K beneath T_c . Depending on the solution under study $\left|\frac{d\Delta\nu}{dT}\right|$ varied between 10^{-2} and $5 \cdot 10^{-3} \text{ Hz} \cdot \text{K}^{-1}$. b_E , the linewidth without chemical exchange was calculated from the low temperature spectra and a reference line, by assuming $\frac{b_E^{\text{ref}}}{b_E}$ independent of temperature. The b_E values were found between 1.0 and 2.0 Hz. A definite pressure dependence of b_E was not observed. Since rising pressure leads to a decrease of the molecular mobility and thus increases the transversal relaxation time T_2 , one can derive from this observation, that the experimental linewidth is mainly determined by external magnetic field inhom-

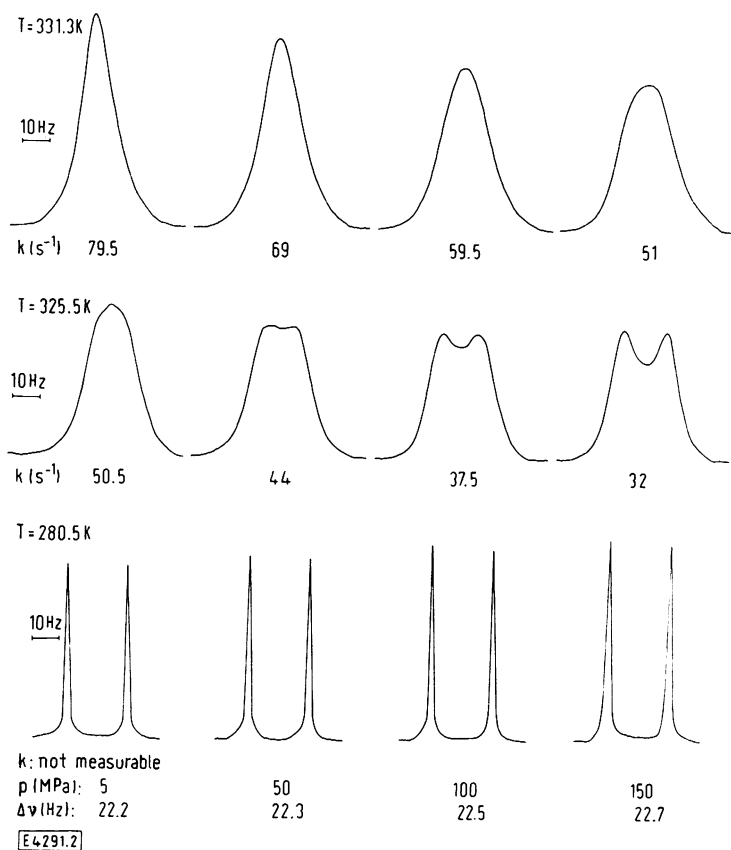


Fig. 2

Temperature and pressure dependence of the proton signals of the two N-methylgroups in neat DMiBu. (k : inversion rate derived from the computer simulation, $\Delta\nu$: chemical shift difference)

genetics and unresolved J -couplings ($T_2 > T_2^*$). Details of the procedure are described in the previous paper [1]. Given the quality of the high pressure spectra, errors in $\Delta\nu$ and/or $b_E \leq 0.3$ Hz could not be resolved by comparison of the simulated and experimental, exchange broadened spectra. In the range of $\Delta\nu/b_E$ covered by our experiments, this uncertainty would lead to a maximal error of 1% (≈ 1 kJ \cdot mol $^{-1}$) for ΔG^\ddagger and of 10% (≈ 1 cm $^3 \cdot$ mol $^{-1}$) for ΔV^\ddagger .

Theoretical

The analysis of the temperature dependence of exchange broadened high resolution NMR-spectra has become the most prominent method for the determination of the rate constant k for intramolecular rearrangements [13]. From the temperature dependence of k , the activation parameters ΔG^\ddagger , ΔH^\ddagger , and ΔS^\ddagger are derived. The accurate determination of ΔH^\ddagger and ΔS^\ddagger depends upon the exact determination of k in a wide range of temperatures and must necessarily cover regions, where the influence of the exchange process upon the spectra is at best marginal. So the results do necessarily carry large errors [14].

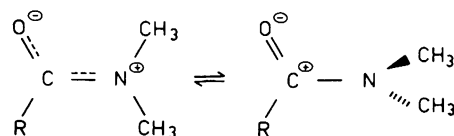
The activation volume ΔV^\ddagger is defined by

$$\left(\frac{\partial \ln k}{\partial p}\right)_T = -\frac{\Delta V^\ddagger}{RT}$$

and can be derived from the analysis of a single high pressure isotherm, in a temperature region where the appearance of the spectra is very sensitive to changes in the inversion rate. The mechanistic information extractable from ΔV^\ddagger is often complementary to the informations that can be gathered from ΔS^\ddagger [15, 16].

The activation volume for the inversion of the N,N-dimethylamides in all solvents, except water, is around +10 cm $^3 \cdot$ mol $^{-1}$. In the highly polar ground state the six atoms of the amide group and its next substituents lie within a plane. This planar form is stabilized by π -electron delocalisation from the carbonyl bond into the amide N–C(=O)-bond. This electronic configuration explains the high electric dipole-moment of the N,N-dimethylamide group of ≈ 3.8 Debye, as well as the high free activation enthalpies for the inversion observed. In the transition state this charge

delocalisation is no longer possible. Here the dimethylaminogroup is twisted 90° out of the plane and thus the polarity must be significantly reduced.



Two different explanations have been given for the sign and magnitude of the activation volume found experimentally. Our group preferred as a working hypothesis a simple sterical model [1], while leNoble [15, 17] proposed, that the reduction of electrostriction in the transition state is responsible for the volume effects observed.

Results

Fig. 2 gives a representative example of the effect of pressure upon the proton signals of the two N-methylgroups in DMiBu(neat). The temperature where the two signals first merge into one exchange broadened signal is called the coalescence temperature T_c . Under the assumption, that ΔS^\ddagger is equal to zero, one can derive the inversion rate k and the free activation enthalpy ΔG^\ddagger from T_c , $\Delta\nu_c$

Table 2
Coalescence temperatures T_c and chemical shift differences $\Delta\nu$ in the system DMB/D $_2$ O

x_{D_2O}	w/w-% DMB	w/w-% D $_2$ O	w/w-% deut.	P MPa	T_c K	$\Delta\nu_c$ Hz
0.999	0.6	99.4	95.5	5	347.8	12.3
				50	348.1	12.0
				100	348.4	11.7
				150	348.7	11.3
0.996	2.8	97.2	90.9	5	348.8	14.6
				50	349.6	14.3
				100	350.2	14.0
				150	350.6	13.7
0.994	4.6	95.4	90.9	5	345.7	16.0
				50	346.6	15.6
				100	347.7	15.4
				150	349.0	15.3
0.987	9.3	90.7	90.9	5	345.2	20.6
				50	346.7	20.3
				100	348.0	20.0
				150	349.0	19.7
0.971	19.3	80.7	52.5	5	337.4	20.6
				50	339.7	20.2
				100	341.9	20.0
				150	342.7	19.8
0.920	40.1	59.9	76.8	5	330.2	24.4
				50	332.2	24.1
				100	333.7	23.8
				150	— **)	23.6
0.688	79.0	21.0	0	5	319.7	25.4
				50	322.2	25.4
				100	324.2	25.4
				150	325.7	25.4
0.516	88.6	11.4	0	5	307.2	22.0
				50	308.9	21.8
				100	310.8	21.7
				150	312.9	21.6
0	22.3*)	0	0	5	295.9	39.8
				50	298.4	40.4
				100	300.3	41.2
				150	302.2	41.7

*) 77.7 w/w-% benzene, Ref. [1].

***) Phase separation.

Table 1

Coalescence temperatures T_c and chemical shift differences $\Delta\nu$ in the system DMA/D $_2$ O

x_{D_2O}	w/w-% DMA	w/w-% D $_2$ O	w/w-% deut.	P MPa	T_c K	$\Delta\nu_c$ Hz
0.990	4.4	95.6	76.8	5	373.8	15.4
				50	374.0	15.6
				100	374.2	15.7
				150	374.4	15.8
0.954	18.0	82.0	64.8	5	372.4	15.6
				50	372.7	15.7
				100	373.2	15.8
				150	373.7	15.9
0.837	46.5	53.5	76.8	5	371.7	16.3
				50	372.9	16.6
				100	374.4	16.8
				150	375.5	16.9
0.774	56.6	43.4	76.8	5	369.5	16.4
				50	370.7	16.6
				100	372.1	16.8
				150	373.9	17.0
0.564	77.6	22.4	76.8	5	364.8	16.8
				50	365.8	17.0
				100	367.7	17.2
				150	369.7	17.3
0	100	0	0	5	351.2	17.2
				50	352.7	17.4
				100	354.7	17.7
				150	356.7	17.9

the chemical shift difference at T_c , and b_E the line width without chemical exchange by standard procedures [18, 19]. The k -values derived by this approximation were used as starting values in the computer lineshape simulation. The final k -values, giving the best fit with the experimental spectra, are given at the bottom of the spectra.

The T_c and Δv_c for two of the systems studied, are given in Table 1 for DMA/ D_2O and in Table 2 for DMF/ D_2O . The other data have been omitted for the sake of brevity from the publication, but are available upon request from the authors.

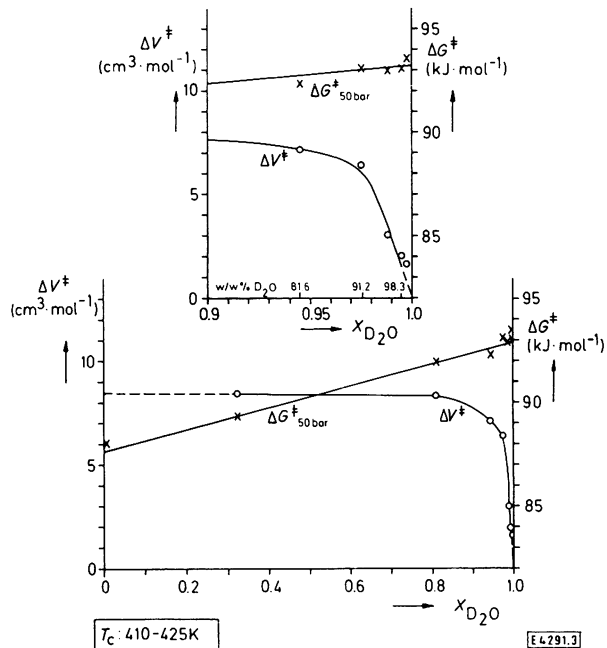


Fig. 3

Activation volumes ΔV^\ddagger and free activation enthalpies ΔG^\ddagger in the system DMF/ D_2O . (The insert at the bottom gives the range of T_c found)

DMF/ D_2O

Fig. 3 and Table 3 summarize the data obtained in these solutions. The free activation enthalpy is increasing linearly with the mole fraction of water. ΔV^\ddagger however remains essentially constant up to $x_{D_2O} \approx 0.9$ and drops in the most dilute solutions very rapidly. The limited experimental sensitivity prohibits the extension of the measurements to smaller amide concentrations.

DMA/ D_2O

Fig. 4, Tables 1, 4, and 5 contain the data for this amide. For the aqueous solutions again an approximately linear increase of ΔG^\ddagger with x_{D_2O} is found. Compared to DMF/ D_2O the decrease in ΔV^\ddagger starts at considerably smaller x_{D_2O} . In the DMA solution with $x_{D_2O} = 0.99$ ΔV^\ddagger is very close to zero. This concentration dependence of ΔV^\ddagger is, to our knowledge, found in the aqueous solutions only. As can be seen in Fig. 4, the solutions of DMA in acetone and

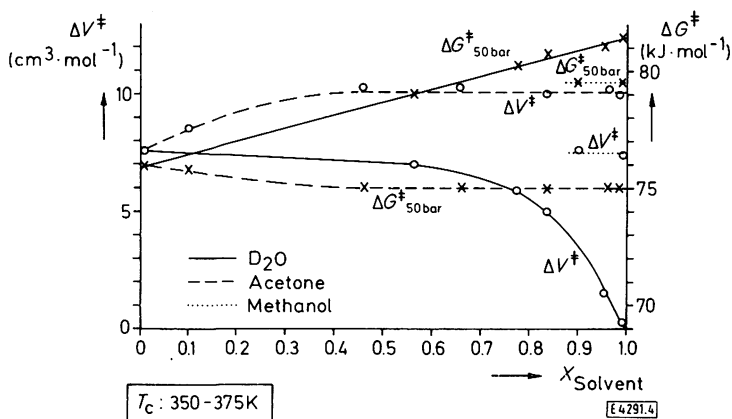


Fig. 4

Activation volumes ΔV^\ddagger and free activation enthalpies ΔG^\ddagger in the systems DMA/ D_2O , DMA/Acetone, DMA/Methanol. (The insert at the bottom gives the range of T_c found)

Table 3
Free activation enthalpies ΔG^\ddagger at 5 MPa and activation volumes ΔV^\ddagger in the system DMF/ D_2O

x_{D_2O}	w/w-% DMF	w/w-% D_2O	w/w-% deut.	$\frac{\Delta G_{5MPa}^\ddagger}{kJ \cdot mol^{-1}}$	$\frac{\Delta G_{lit}^\ddagger}{kJ \cdot mol^{-1}}$	$\frac{\Delta V^\ddagger}{cm^3 \cdot mol^{-1}}$
0.997	1.0	99.0	90.9	93.5		1.6
0.995	1.7	98.3	90.9	93.1		2.0
0.988	4.3	95.7	95.5	93.0		3.0
0.975	8.8	91.2	90.9	93.1		6.4
0.945	18.4	81.6	52.5	92.3		7.1
0.810	46.8	53.2	76.8	91.8		8.3
0.322	89.5	10.5	0	89.3		8.4
0	100	0	0	—	87.5*)	—

*) Ref. [5].

Table 4
Free activation enthalpies ΔG^\ddagger at 5 MPa and activation volumes ΔV^\ddagger in the system DMA/ D_2O

x_{D_2O}	w/w-% DMA	w/w-% D_2O	w/w-% deut.	$\frac{\Delta G_{5MPa}^\ddagger}{kJ \cdot mol^{-1}}$	$\frac{\Delta G_{lit}^\ddagger}{kJ \cdot mol^{-1}}$	$\frac{\Delta V^\ddagger}{cm^3 \cdot mol^{-1}}$
0.990	4.4	95.6	76.8	81.4		0.3
0.954	18.0	82.0	64.8	81.0	80.8*)	1.5
0.837	46.5	53.5	76.8	80.7		5.0
0.774	56.6	43.4	76.8	80.2		5.9
0.564	77.6	22.4	76.8	79.2		7.0
0	100	0	0	75.9	75.8**)	7.6

*) $x_{D_2O} = 0.9$, Ref. [5].

***) Ref. [5].

Table 5
Free activation enthalpies ΔG^* at 5 MPa and activation volumes ΔV^\ddagger in the systems DMA/Acetone and DMA/Methanol

x_{Solvent}	w/w-% DMA	w/w-% Solvent	w/w-% deut.	$\frac{\Delta G_{5\text{MPa}}^*}{\text{kJ} \cdot \text{mol}^{-1}}$	$\frac{\Delta G_{\text{lit}}^*}{\text{kJ} \cdot \text{mol}^{-1}}$	$\frac{\Delta V^\ddagger}{\text{cm}^3 \cdot \text{mol}^{-1}}$
Acetone						
0.985	2.0	98.0	90.0	75.0	75.4*)	10.0
0.963	5.0	95.0	90.0	75.0		10.2
0.836	21.0	79.0	99.1	75.0		10.0
0.657	41.5	58.5	99.1	75.0		10.3
0.460	61.5	38.5	99.1	75.0		10.3
0.099	93.2	6.8	0	75.8		8.5
Methanol						
0.992	2.0	98.0	90.1	79.6		7.4
0.902	20.8	79.2	99.0	79.5		7.6

*) $x_{\text{Acetone}} = 0.9$, Ref. [5].

Table 6
Free activation enthalpies ΔG^* at 5 MPa and activation volumes ΔV^\ddagger in the system DMPPr/D₂O

$x_{\text{D}_2\text{O}}$	w/w-% DMPPr	w/w-% D ₂ O	w/w-% deut.	$\frac{\Delta G_{5\text{MPa}}^*}{\text{kJ} \cdot \text{mol}^{-1}}$	$\frac{\Delta G_{\text{lit}}^*}{\text{kJ} \cdot \text{mol}^{-1}}$	$\frac{\Delta V^\ddagger}{\text{cm}^3 \cdot \text{mol}^{-1}}$
0.998	1.0	99.0	90.9	78.9		2.1
0.996	1.8	98.2	90.9	78.6		2.3
0.991	4.2	95.8	95.5	78.5		6.3
0.960	17.4	82.6	90.9	78.5		7.6
0.882	41.7	58.3	52.5	77.2		8.6
0.723	67.1	32.9	52.5	76.6		9.4
0.404	89.2	10.8	0	74.1		9.2
0	95*)	0	0	72.5	72.0**)	8.6

*) 5 w/w-% hexamethyldisiloxane.

***) Ref. [5, 20].

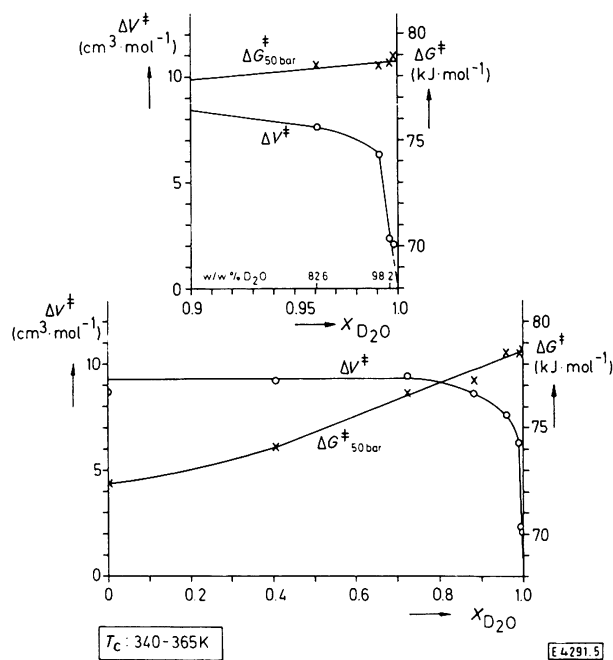


Fig. 5

Activation volumes ΔV^\ddagger and free activation enthalpies ΔG^\ddagger in the system DMPPr/D₂O. (The insert at the bottom gives the range of T_c found)

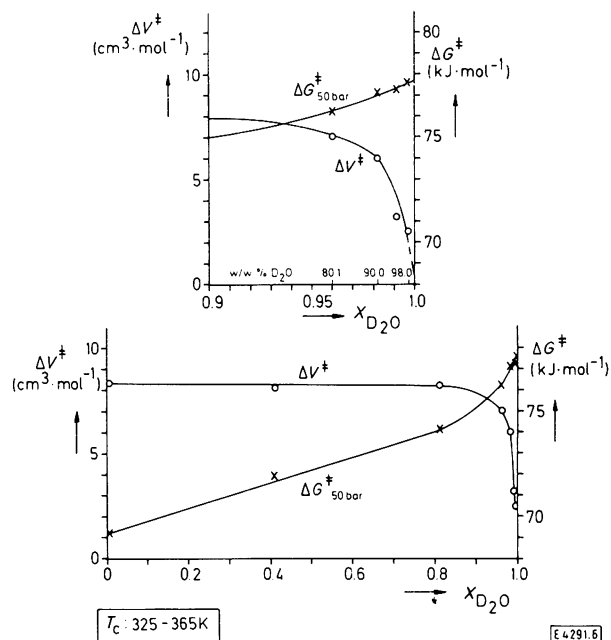


Fig. 6

Activation volumes ΔV^\ddagger and free activation enthalpies ΔG^\ddagger in the system DMiBu/D₂O. (The insert at the bottom gives the range of T_c found)

Table 7
Free activation enthalpies ΔG^* at 5 MPa and activation volumes ΔV^* in the system DMiBu/D₂O

x_{D_2O}	w/w-% DMiBu	w/w-% D ₂ O	w/w-% deut.	$\frac{\Delta G_{5MPa}^*}{kJ \cdot mol^{-1}}$	$\frac{\Delta G_{lit.}^*}{kJ \cdot mol^{-1}}$	$\frac{\Delta V^*}{cm^3 \cdot mol^{-1}}$
0.997	2.0	98.0	90.9	77.6		2.5
0.991	5.0	95.0	90.9	77.2		3.2
0.982	10.0	90.0	76.8	77.1		6.0
0.960	19.9	80.1	76.8	76.2		7.0
0.811	58.9	41.1	52.5	74.1		8.2
0.418	95.0	5.0	0	71.9		8.1
0	100	0	0	69.2	69.1*)	8.3

*) Ref. [5, 20].

Table 8
Free activation enthalpies ΔG^* at 5 MPa and activation volumes ΔV^* in the system DMV/D₂O

x_{D_2O}	w/w-% DMV	w/w-% D ₂ O	w/w-% deut.	$\frac{\Delta G_{5MPa}^*}{kJ \cdot mol^{-1}}$	$\frac{\Delta G_{lit.}^*}{kJ \cdot mol^{-1}}$	$\frac{\Delta V^*}{cm^3 \cdot mol^{-1}}$
0.999	1.0	99.0	90.9	79.5		4.0
0.996	2.3	97.7	90.9	79.4		5.1
0.992	5.0	95.0	90.9	79.1		6.5
0.964	19.9	80.1	76.8	77.7		7.5
0.913	39.5	60.5	52.5	77.0		8.4
0.526	86.6	13.4	0	74.7		8.7
0	95*)	0	0	72.1		8.9

*) 5 w/w-% hexamethyldisiloxane.

methanol do not show any significant change of the free activation enthalpy or the activation volume in the high dilution range.

DMPPr/D₂O

The addition of a further methylene group to the carbonyl-substituent lowers ΔG^* in the dilute solutions by approximately $3 kJ \cdot mol^{-1}$ compared to DMA. The results found in these mixtures are collected in Fig. 5 and Table 6. The decrease in ΔV^* begins, compared to DMF/D₂O and DMA/D₂O, at significantly higher x_{D_2O} .

DMiBu/D₂O

The activation volumes derived (cf. Fig. 6 and Table 7) show a similar concentration dependence for ΔV^* as observed in DMPPr/D₂O. In this system however, also the ΔG^* versus x_{D_2O} curve shows a pronounced deviation from linearity. The slope becoming considerably steeper in the water rich region.

DMV/D₂O

This amide shows a behaviour qualitative similar to DMPPr/D₂O (cf. Fig. 7 and Table 8).

Among the compounds described hitherto, the results obtained in DMF/D₂O are not directly comparable to the other four systems, since the accurate extraction of inversion rates from the exchange broadened spectra is limited to the temperature region $T_c \pm 10 K$. The high ΔG^* of DMF thus restricts the analysis of the spectra to temperatures around 415 K, while the systems of DMA, DMPPr, DMiBu, and DMV can be studied in the dilute solutions at $350 \leq T \leq 375 K$. Within this limited ranges no temperature dependence of ΔV^* is detectable.

DMB/D₂O

Here a dimethylamide with an aromatic substituent at the carbonyl group has been included into the studies. The results

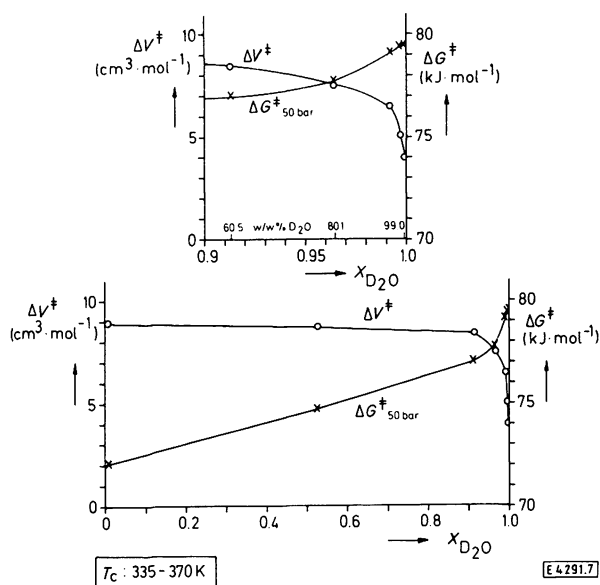


Fig. 7
Activation volumes ΔV^* and free activation enthalpies ΔG^* in the system DMV/D₂O. (The insert at the bottom gives the range of T_c found)

are given in Fig. 8 and Table 9. At temperatures $> 340 K$ and $x_{D_2O} \approx 0.9$ this system shows phase separation into two liquid phases, the two-phase region extending with increasing pressure to lower temperatures. The deviation of the ΔV^* versus x_{D_2O} curve from linearity is most pronounced for this compound. ΔV^* is essentially concentration independent up to $x_{D_2O} = 0.97$ and falls very rapidly at higher dilutions. The increase of ΔG^* with concentration amounts to $15 kJ \cdot mol^{-1}$, almost twice the change observed in any aliphatic amide.

Table 9
Free activation enthalpies ΔG^* at 5 MPa and activation volumes ΔV^* in the system DMB/ D_2O

x_{D_2O}	w/w-% DMB	w/w-% D_2O	w/w-% deut.	$\frac{\Delta G_{5MPa}^*}{kJ \cdot mol^{-1}}$	$\frac{\Delta G_{lit.}^*}{kJ \cdot mol^{-1}}$	$\frac{\Delta V^*}{cm^3 \cdot mol^{-1}}$
0.999	0.6	99.4	95.5	76.3		3.0
0.996	2.8	97.2	90.9	75.9		4.5
0.994	4.6	95.4	90.9	74.9	75.7**)	5.5
0.987	9.3	90.7	90.9	74.0		6.8
0.971	19.3	80.7	52.5	72.3		8.9
0.920	40.1	59.9	76.8	70.3		8.9
0.688	79.0	21.0	0	67.8		9.0
0.516	88.6	11.4	0	65.5		8.9
0	22.3*)	0	0	61.5	61.5***)	8.1

*) 77.7 w/w-% benzene, Ref. [1].

** $x_{D_2O} = 0.991$, Ref. [4].

***) Ref. [4].

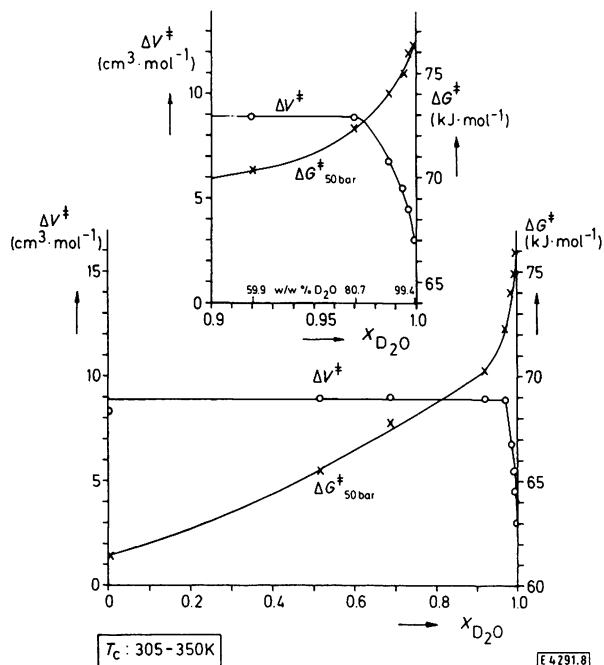


Fig. 8

Activation volumes ΔV^* and free activation enthalpies ΔG^* in the system DMB/ D_2O . (The insert at the bottom gives the range of T_c found)

Discussion

It is not the intention of the present paper to renew the discussion about the solvent influence upon the free activation enthalpy. Excellent reviews about this subject can be found in the literature [5, 6, 21]. The strong increase of ΔG^* in the aqueous solutions with decreasing concentration of the amide, can definitely not be explained by a change of the bulk electrostatic interaction of the molecule with the surrounding liquid phase, since neither the dipole moments of the solvent molecules, nor the static dielectric constant of the solvent do correlate quantitatively with the variations observed for ΔG^* [1, 4–6, 21]. The protic solvents do show the largest increase of ΔG^* . This is generally explained by the formation of a hydrogen bond between the carbonyl oxygen and the polar hydrogens of the solvent [6, 21], which preferably stabilizes the polar ground state by balancing part of the excess negative charge on the carbonyl oxygen atom.

The pronounced decrease of ΔV^* in the dilute solutions of the dimethylamides is, according to our knowledge, found

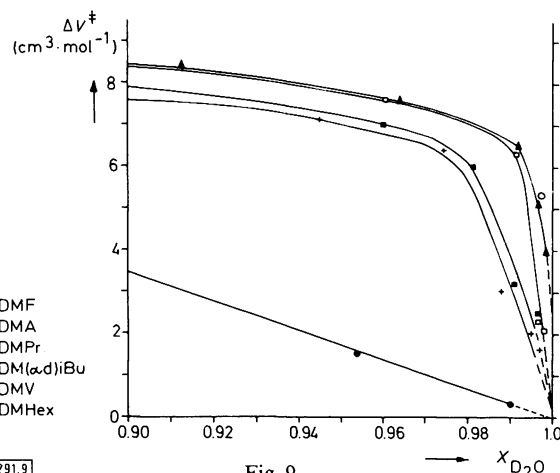


Fig. 9

Activation volumes in the water rich regions of the aqueous solutions of the aliphatic amides. (In addition to the systems described above, a single measurement on *N,N*-Dimethylhexanoicamide has been included $x_{D_2O} = 0.997$; $\Delta G^* = 79.3 kJ \cdot mol^{-1}$; $\Delta V^* = 5.3 cm^3 \cdot mol^{-1}$)

only in the aqueous solutions. The data obtained in the dilute solutions are shown on an expanded scale in Fig. 9. It is an additional experimental evidence for the general observation, that many solute and solvent properties of the aqueous solutions of nonelectrolyte molecules do show a strong concentration dependence, even in the most dilute regions [22]. According to Franks [24], this can only be rationalized, if the solute is not randomly distributed in the water, but shows even at the highest dilutions, accessible to experiment, microheterogeneous distributions. Evidence for this microheterogeneities have been found in longitudinal relaxation rate studies of the aqueous solutions of formamide, *N*-methylformamide and *N,N*-dimethylformamide [25, 26]. In these systems the deviation of the correlation times and the self diffusion coefficients from regular solution behavior increases with the hydrophobic character of the solute. The same effect is observed for the dimethylamides investigated here:

The drop of the activation volume is shifted with increasing size of the unpolar residues to higher x_{D_2O} . This is a strong hint, that hydrophobic interaction is responsible for the microheterogeneous distribution of the amides in water. Hydrophobic interaction is an entropy driven process [24] and should thus become more pronounced with rising temperature. Experimentally we observe, that DMB and

DMV are completely miscible with water near room temperature, but do show macroscopic phase separation at elevated temperatures. This is further evidence that the microheterogeneity is enhanced with rising temperature.

The increase of self association of the amide molecules with temperature would also explain, that the decrease of ΔV^\ddagger in the system DMF/D₂O starts at much higher x_{D_2O} , than observed in DMA, since, as explained in the experimental section, the measurements in DMF/D₂O had to be performed at temperatures around 420 K, while the rest of the amides had to be studied around 360 K.

The decrease of ΔV^\ddagger in the high dilution range of the aqueous solutions cannot be derived from the electrostriction model proposed by le Noble [17], since the electrostatic interaction between a central amide molecule and the surrounding solvation shell should not be influenced too severely through the gradual replacement of the amide molecules in the solvation shell by water molecules. Neither does the model proposed by us [1], with a random close packed solvation shell, that has to be expanded before inversion of the dimethylaminogroup can occur, account for the effects observed.

We therefore propose a working hypothesis, to explain the small activation volumes found in the dilute solutions of the dimethylamides:

1. Only at very high dilutions most of the amide molecules are found in isolated and monomeric distribution in water.
2. These hydrated monomers do carry, in the time average, an open hydration shell around the dimethylaminogroup, thus permitting rotation of this group without significant rearrangement of the water molecules in the immediate neighbourhood of the group.

This working hypothesis is corroborated by x-ray studies on simple liquids and clathrates. It is well established, that the radial distribution function of simple liquids and especially of water and ammonia [27, 28], is only slightly changed in the melting process. For instance the number of next neighbours in the liquid water increases only from 4 in ice I to ≈ 4.4 in the melting process. Furthermore the radial distribution function of water changes only marginally when the temperature is raised to 570 K [29]. Dimethylamine in the solid state forms a clathrate like hydrate [30]. Recently Zimmermann et al. [31] showed for the first time, that the radial distribution function of ethyleneoxide, a molecule of similar size and polarity as dimethylamine, in water is compatible with the structure of the solid ethyleneoxide clathrate and that the results of the small angle x-ray scattering experiments are best explained by assuming a relatively free mobility of the ethyleneoxide in the solvent cage. In view of the small changes of the radial distribution function of water with temperature, it appears reasonable to assume, that the solvation structures found close to the melting point do persist to much higher temperatures.

It is obvious that the working hypothesis proposed, can and must be critically analyzed by studying dialkylamides with larger substituents at the nitrogen and/or by investigating amides carrying additional hydroxyl- or aminogroups at the N-alkylresidues.

It is a pleasure to thank Mr. R. Knott and Mr. S. Heyn for their expert technical assistance that made this work feasible.

The spectra simulations were performed at the TR 440 of the computer center of the Universität Regensburg.

Financial support by the Deutsche Forschungsgemeinschaft and the Fonds der Chemischen Industrie is gratefully acknowledged.

References

- [1] R. Rauchschalbe, G. Völkel, E. Lang, and H.-D. Lüdemann, *J. Chem. Res. (S)* 448 (1978), (M) 5325 (1978).
- [2] A. E. Merbach and H. Vanni, *Helv. Chim. Acta* 60, 1124 (1977).
- [3] H.-D. Lüdemann, R. Rauchschalbe, and E. Lang, *Angew. Chem., Int. Ed. Engl.* 16, 331 (1977).
- [4] L. M. Jackman, T. E. Kavanagh, and R. C. Haddon, *Org. Magn. Reson.* 1, 109 (1969).
- [5] T. Drakenberg, K.-I. Dahlqvist, and S. Forsén, *J. Phys. Chem.* 76, 2178 (1972).
- [6] L. M. Jackman, in: L. M. Jackman and F. A. Cotton, eds., *Dynamic Nuclear Magnetic Resonance Spectroscopy*, p. 203 ff., Academic Press, New York 1975.
- [7] L. S. Trzupek, E. R. Stedronsky, and G. M. Whitesides, *J. Org. Chem.* 37, 3300 (1972).
- [8] H. Yamada, *Rev. Sci. Instruments* 45, 690 (1974).
- [9] U. Gaarz and H.-D. Lüdemann, *Ber. Bunsenges. Phys. Chem.* 80, 607 (1976).
- [10] E. Lang, R. Rauchschalbe, and H.-D. Lüdemann, *High Temperatures-High Pressures* 9, 519 (1977).
- [11] D. S. Stephenson and G. Binsch, *J. Magn. Reson.* 32, 145 (1978).
- [12] V. Jonas, Ph. D. Thesis UC Riverside, p. 226 (1970).
- [13] L. M. Jackman and F. A. Cotton, *Dynamic Nuclear Magnetic Resonance Spectroscopy*, Academic Press, New York 1975.
- [14] G. Binsch, in: L. M. Jackman and F. A. Cotton, eds., *Dynamic Nuclear Magnetic Resonance Spectroscopy*, p. 45 ff., Academic Press, New York 1975.
- [15] T. Asano and W. J. le Noble, *Chem. Rev.* 78, 407 (1978).
- [16] H. Kelm and D. A. Palmer, in: H. Kelm, ed., *High Pressure Chemistry*, p. 281 ff., Reidel Publishing Company, Dordrecht 1977.
- [17] W. J. le Noble, in: H. Kelm, ed., *High Pressure Chemistry*, p. 325 ff., Reidel Publishing Company, Dordrecht 1977.
- [18] H. Friebolin, *NMR-Spektroskopie*, p. 79 ff., Verlag Chemie, Weinheim 1974.
- [19] H. Günther, *NMR-Spektroskopie*, p. 247, Georg Thieme, Stuttgart 1973.
- [20] M. D. Wunderlich, L. K. Leung, J. A. Sandberg, K. D. Meyer, and C. H. Yoder, *J. Am. Chem. Soc.* 100, 1500 (1978).
- [21] W. E. Stewart and T. H. Siddall, *Chem. Rev.* 70, 517 (1970).
- [22] F. Franks and D. S. Reid, in: F. Franks, ed., *Water - A Comprehensive Treatise*, Vol. 2, p. 323 ff., Plenum Press, New York 1973.
- [23] A. Hvidt, *J. Theor. Biol.* 50, 245 (1975).
- [24] F. Franks, in: F. Franks, ed., *Water - A Comprehensive Treatise*, Vol. 4, p. 1 ff., Plenum Press, New York 1975.
- [25] A. Fratiello, *Mol. Phys.* 7, 565 (1963).
- [26] H. Weingärtner, M. Holz, and H. G. Hertz, *J. Sol. Chem.* 7, 689 (1978).
- [27] A. H. Narten, M. D. Danford, and H. A. Levy, *Discuss. Faraday Soc.* 43, 97 (1967).
- [28] A. H. Narten, *J. Chem. Phys.* 66, 3117 (1977).
- [29] A. H. Narten and H. A. Levy, in: F. Franks, ed., *Water - A Comprehensive Treatise*, Vol. 1, p. 311 ff., Plenum Press, New York 1972.
- [30] R. K. McMullan, T. H. Jordan, and G. A. Jeffrey, *J. Chem. Phys.* 47, 1218 (1967).
- [31] E. Wagner, J.-U. Weidner, and H. W. Zimmermann, *Ber. Bunsenges. Phys. Chem.* 81, 1143 (1977).

(Eingegangen am 16. März 1979) E 4291